Cells
Tissues
Organs

Research Article

Cells Tissues Organs
DOI: 10.1159/000510297

Received: April 20, 2020
Accepted: July 20, 2020
Published online: October 9, 2020

Optimizing the Decellularized Porcine Liver Scaffold Protocol

Lanuza Alaby Pinheiro Faccioli[a, c] Grazielle Suhett Dias[a, b]
Victor Hoff[a] Marlon Lemos Dias[a] Cibele Ferreira Pimentel[a]
Camila Hochman-Mendez[e] Daniella Braz Parente[c, d] Ester Labrunie[c]
Paulo Aantonio Souza Mourão[h] Paolo Rogério de Oliveira Salvalaggio[b]
Anna Carla Goldberg[b] Antonio Carlos Campos de Carvalho[a, f, g]
Regina Coeli dos Santos Goldenberg[a, f]

[a]Cellular and Molecular Cardiology Laboratory, Carlos Chagas Filho Biophysics Institute, Federal University of Rio de Janeiro, Rio de Janeiro, Brazil; [b]Research and Education Institute, Hospital Israelita Albert Einstein, São Paulo, Brazil; [c]Radiology Department, Clementino Fraga Filho University Hospital, Federal University of Rio de Janeiro, Rio de Janeiro, Brazil; [d]D'Or Institute for Research and Education, Botafogo, Rio de Janeiro, Brazil; [e]Texas Heart Institute, Houston, TX, USA; [f]Institute of Science and Technology for Regenerative Medicine – REGENERA, Federal University of Rio de Janeiro, Rio de Janeiro, Brazil; [g]National Center for Structural Biology and Bioimaging – CENABIO, Federal University of Rio de Janeiro, Rio de Janeiro, Brazil; [h]Connective Tissue Laboratory, Clementino Fraga Filho University Hospital, Federal University of Rio de Janeiro, Rio de Janeiro, Brazil

Keywords
Decellularization · Porcine liver · Sodium deoxycholate · HepG2 cells

Abstract
There are few existing methods for shortening the decellularization period for a human-sized whole-liver scaffold. Here, we describe a protocol that enables effective decellularization of the liver obtained from pigs weigh 120 ± 4.2 kg within 72 h. Porcine livers (approx. 1.5 kg) were decellularized for 3 days using a combination of chemical and enzymatic decellularization agents. After trypsin, sodium deoxycholate, and Triton X-100 perfusion, the porcine livers were completely translucent. Our protocol was efficient to promote cell removal, the preservation of extracellular matrix (ECM) components, and vascular tree integrity. In conclusion, our protocol is efficient to promote human-sized whole-liver scaffold decellularization and thus useful to generate bioengineered livers to overcome the shortage of organs.

Introduction

Liver transplantation is the treatment of choice for patients with end-stage liver disease; however, this approach is still limited by several factors, particularly the chronic shortage of donor organs worldwide [Johnson et al., 2014]. Organ incompatibility-associated problems further exacerbate the unmet need for organs [Zhang et al., 2018]. Alternative strategies are needed to increase the number of donor organs available. Bioengineered liver replacements are a promising alternative to existing strategies, such as synthetic mesh components, but they are

karger@karger.com
www.karger.com/cto

Regina Coeli dos Santos Goldenberg
Cellular and Molecular Cardiology Laboratory, Carlos Chagas Filho Biophysics Institute, Federal University of Rio de Janeiro
Carlos Chagas Filho Avenue 373, Ilha do Fundão
Rio de Janeiro, 21941-902 (Brazil)

difficult to produce and do not adequately account for hepatic complexity. In recent years, decellularized porcine livers have emerged as a promising alternative source of organ replacements for liver transplantation, particularly owing to the widespread availability of pig organs and their dimensional and structural compatibility with the human liver [Cooper et al., 2016]. The decellularized porcine liver forms a biocompatible scaffold representing an ideal microenvironment where human liver cells can maintain their phenotype and functionality [Faulk et al., 2015; Mußbach et al., 2016; Wang et al., 2017].

Several studies have demonstrated decellularization of the liver [Baptista et al., 2011; Mirmalek-Sani et al., 2013; Wang et al., 2017; Ansari et al., 2020; Willemse et al., 2020] and others tissues [Burk et al., 2014] obtained from various animal sources. Different methods are used for the decellularization of solid tissues, such as physical disruption [Burk et al., 2014; Nonaka et al., 2014], enzymatic treatment [Rieder et al., 2004; Yang et al., 2009], and applying detergents such as Triton X-100 [Willemse et al., 2020], sodium dodecyl sulfate (SDS) [Ott et al., 2008; Price et al., 2010; Lang et al., 2011; Sullivan et al., 2012; Bühler et al., 2015; Jakus et al., 2017; Pla-Palacín et al., 2017], and sodium deoxycholate (SD) [Ceborati et al., 2010; Remlinger et al., 2012]. However, there are only a few established protocols for decellularization using full-size livers from pigs (that weigh >100 kg) in a short period (<6 days) [Barakat et al., 2012; Remlinger et al., 2012; Ko et al., 2015]. Moreover, there is no consensus about the most effective detergent to decellularize entire porcine livers in the same short period [Lin et al., 2004], which greatly limits the feasibility of the approach for its translation into clinical use. Decellularization of a whole porcine liver (that weighs approx. 1.5 kg) is a significant challenge for 3-dimensional (3D) organ engineering. The long duration of the procedure to remove most of the cellular and immunogenic content of the scaffold may impair extracellular matrix (ECM) composition and 3D architecture. The decellularization method must maintain the integrity of specific epitopes to permit the repopulation process. Therefore, the choice of the detergent and techniques to be used are important steps to ensure future repopulation after decellularization [Faulk et al., 2015].

In this study, we established and described a protocol that enables effective decellularization of the entire porcine (human-size) liver (weight 1.5 kg) obtained from pigs weighing 120 ± 4.2 kg in a short period of time, i.e., 3 days.

So far, most experimental decellularization protocols include the use of sodium dodecyl sulfate (SDS), but this also destroys the ECM and limits the feasibility of the approach for clinical trials [Rotunda et al., 2004]. We established a modified protocol using an ionic decellularization detergent that has not been widely utilized in other protocols, is less aggressive, and increases the viability of the approach for translation into clinical use [Rotunda et al., 2004]. SD removes all liver cells while maintaining the ECM integrity and keeping the vascular tree components intact. In addition, our liver scaffold is clinically relevant for use in split-liver transplantation that can benefit ≥2 patients.

Materials and Methods

Porcine Liver Preparation

Nonischemic livers were removed from pigs weighing 120 ± 4.2 kg (n = 3). All livers were recovered after transplant surgery training courses using pigs, at the institution's Animal Facility. Briefly, after the animal was sacrificed by means of potassium chloride, the abdominal cavity was opened through a long midline incision, and the portal vein and hepatic pedicle were skeletonized and dissected up to the upper border of the pancreas and cannulated. The livers were removed and stored dry at –80 °C prior to decellularization.

Decellularization Protocol for Whole Porcine Liver

Our protocol for whole porcine liver decellularization was based on anterograde perfusion through the portal vein. Figure 1 details the perfusion protocol. We used the following reagents: Triton X-100 (Sigma-Aldrich, T9284), trypsin (Sigma-Aldrich, T4799), PBS (LGC, 13–3025805, São Paulo, Brazil), and SD (Sigma-Aldrich, P6750). A peristaltic pump (Masterflex, Cole Parmer L/S, model 7519-05) was used and the initial flow rate for decellularization was 50 mL/min. Subsequently, a perfusion-modified protocol was adopted. Distilled water was perfused to wash the blood for 1 h, followed by 2× PBS for 1 h and then 0.2% trypsin solution in 0.05% EDTA (Sigma-Aldrich, 600-04) and 0.05% NaN_3 (Sigma-Aldrich, 26628-228) for 12 h at 37 °C. Afterwards, 3% Triton X-100 solution in 0.05% EDTA and 0.05% NaN_3 was perfused for 24 h and finished with 4% SD solution for 34 h [Ceborati et al., 2010].

Histology

Decellularized porcine liver scaffolds were dissected to perform characterization. The samples (n = 4) were taken from different sites of the decellularized liver scaffold. Liver samples were fixed in 10% formalin for 24 h. Samples were then embedded in Paraplast and sections were cut in slices at a thickness of approximately 5 µm using a microtome. These sections were stained with hematoxylin and eosin (H&E) and Sirius red.

Vascular Tree Integrity

The integrity of the vascular system in the decellularized liver scaffold was evaluated by digital subtraction angiography (DSA). Iodine contrast agent (100 mL; Henetix®, Guerbet, 350 mg/mL) was infused through the portal vein and via the intrahepatic vena cava to detect the distribution.

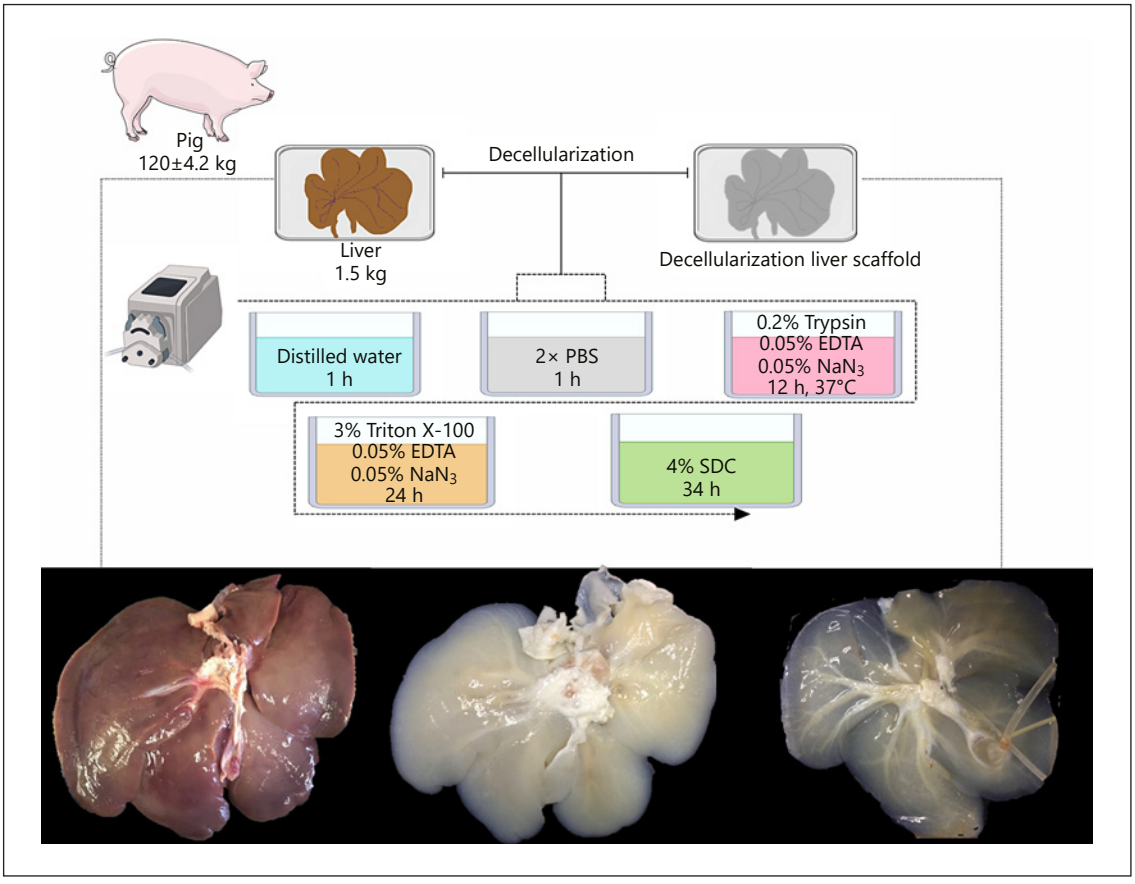

Fig. 1. Schematic experimental design. Porcine liver weighting approximately 1.5 kg is surgically processed, cannulated and decellularized by anterograde perfusion according to SD protocol. Post 72 h of perfusion, decellularized liver scaffold is obtained.

DNA Analysis

DNA was isolated from a small piece of the decellularized porcine liver scaffold and the 3 porcine livers with cells using the DNeasy tissue kit (Qiagen Inc., Valencia, CA, USA) according to the manufacturer's instructions. Similar masses of scaffold and control liver tissue were used. DNA concentration was determined by measuring the absorbance at 260 nm using NanoDrop 1000 (Thermo Scientific). Data were averaged and expressed as mean + standard deviation.

Immunohistochemistry

For immunohistochemical analysis, paraffin-embedded sections (4 samples per liver) of the decellularized liver were unmasked in citrate acid solution at pH 6.0 for 12 min in a microwave oven at 700 W. Afterwards, the scaffolds were blocked with albumin and then incubated with 1 of the following primary antibodies: anti-collagen III (Chemicon, USA; 1:100) or anti-collagen IV (Sigma, USA; 1:100). All sections were incubated with HRP-conjugated secondary antibody (for more information, see in online suppl. Table 1; for all online suppl. material, see www.karger.com/doi/10.1159/000510297) and detection was performed using reagents indicated by the manufacturer (EnVision Doublestain System, Dako, USA). Sections were stained with H&E. Images were obtained with an AxioCam camera using KS400 software (Zeiss, Germany).

Glycosaminoglycan Quantification

For chemical determination of the total glycosaminoglycan (GAG) content after decellularization, 4 samples of each liver (controls and decellularized) were cut into small pieces (1 mm). and submerged in chloroform/methanol (2:1, v/v) for 10 min for delipidation, and then dried at 60 °C for 2 days and weighed. Dry tissue (0.05 g) was set aside for determining the GAG content by measuring the amount of hexuronic acid by means of the carbazole reaction, as described elsewhere [Bellezzia et al., 2018]. GAG concentration was determined by measuring the absorbance at 525 nm using a spectrophotometer (Nova Instruments Serie 1800). Data were averaged and expressed as mean ± standard deviation.

Scanning Electron Microscopy

Liver samples were fixed in 4% Karnovsky solution using intact fragments for evaluation of the liver surface. Samples were fixed in 1% osmium tetroxide, dehydrated with an increasing series of ethyl alcohol, set up in stubs, and metallized with gold. Observations

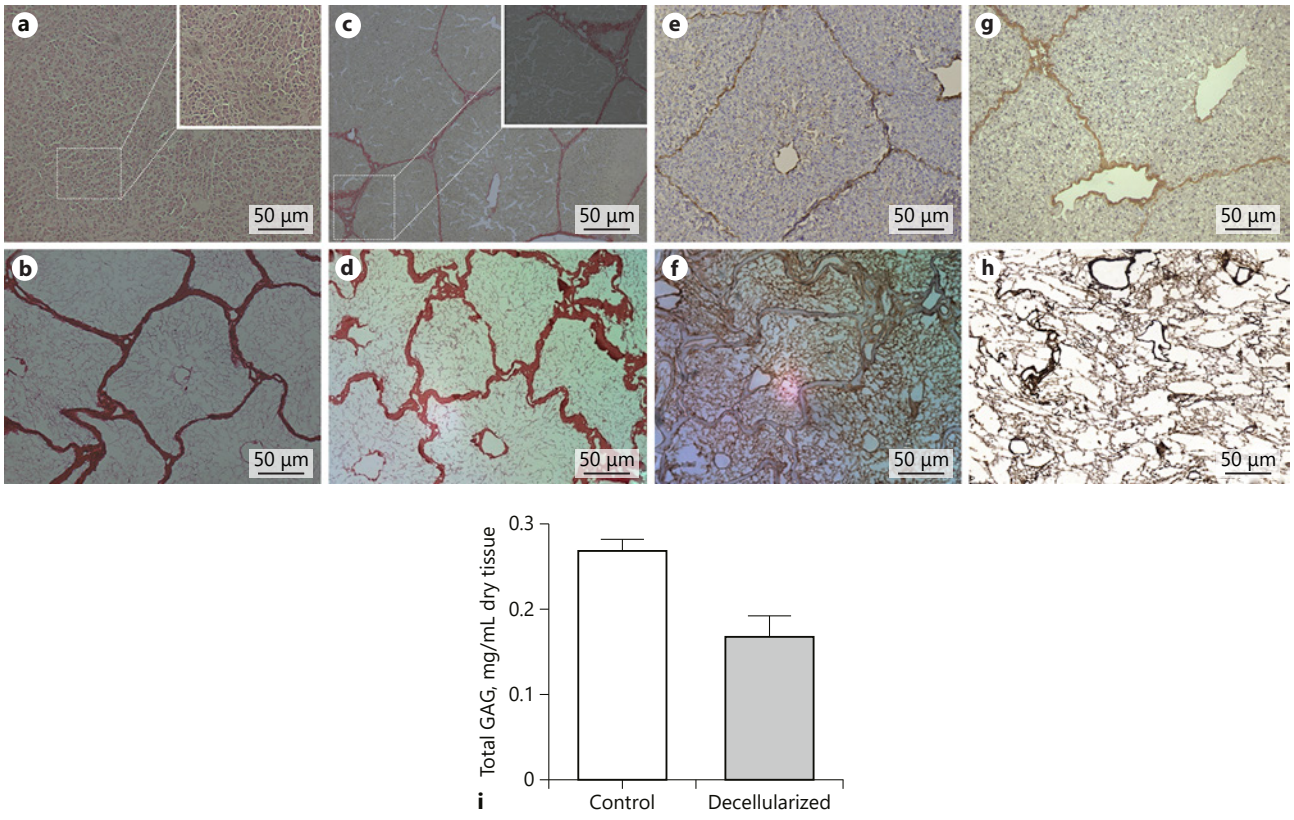

Fig. 2. Histological and immunohistochemical analysis of normal and decellularized porcine livers and total GAG quantification. **a** H&E staining showing the presence of hepatic cells nuclei in normal liver tissue. **b** Absence of cells in liver tissue decellularized with SD. Central veins are present in both normal and decellularized SD livers. Sirius red staining shows the collagen deposition in normal livers (**c**) and decellularized SD livers (**d**). **e**, **g** Tissue sections of normal porcine liver tissue showing positive brown staining for collagen type III and IV. **f**, **h** The positive brown staining for collagen was also present in the decellularized tissues, indicating that these processes did not have a major effect on the extracellular matrix (ECM). **i** GAG quantification shows no significant reductions in GAG content in decellularized tissue compared to the normal liver. Each bar represents pooled data obtained from 3 pigs per group.

and photographs were performed using a scanning electron microscope (Zeiss [LEO] model 435VP, 20kV).

Transmission Electron Microscopy

Liver fragments were fixed in 2.5% glutaraldehyde. Tissues were further fixed in the same solution for 12 h at 4 °C. The specimens were postfixed in 2% osmium tetroxide solution, rinsed in distilled water, and immersed in 2% tannic acid solution for 1 h at room temperature. Tissues were then dehydrated in a series of increasing levels of ethanol and propylene oxide and embedded in Spurr resin. Thick sections were obtained with a Porter Blum ultramicrotome using glass knives and stained with Toluidine blue solution for light microscopy. A Reichert ultramicrotome (Leica) with a diamond knife was used to cut the thin sections. These ultrathin sections were mounted on 200- and 300-mesh grids, counterstained with uranyl acetate and lead citrate, and then examined with a transmission electron microscope (JEOL, JSM1010 at 100 kV).

Cell Seeding

Liver tissue was cut into 300-μm slices by means of a microtome (Leica, USA). We divided it into 3 groups. The positive control consisted of hepatocyte carcinoma cells (HepG2) cultured without the matrix. The negative control consisted of 3 slices cultured without HepG2 cells. The experimental group consisted of HepG2 cells cocultured with 3 slices of the matrix. All slices were sterilized with a solution of penicillin and streptavidin 1% (Invitrogen, USA) for 24 h. HepG2 cells were cultured in a 100-mm plate for 5 days. After that, cells were trypsinized and counted manually. The amount of 2×10^6 cells were cultured over the experimental slice and 2×10^6 cells were cultured for the positive control in a nonadherent culture lamina (HEXIS, USA), with DMEM high medium (Sigma), 15% FBS (Sigma), and 1% penicillin and streptavidin (Invitrogen, USA) for 7 days. The medium was changed every 2 days.

Immunofluorescence

Three samples from each group were fixed in 4% paraformaldehyde for 20 min at room temperature. Primary anti-albumin antibody (1:1,000; Abcam) was used after three 10-min permeabilizations with 0.3% Triton X-100 in PBS, and then incubated overnight at 4 °C. Samples were washed and incubated for 2 h at room temperature with donkey anti-sheep Alexa Fluor 488 (1:400; Invitrogen) secondary antibody (online suppl. Table 1). For staining the nuclei, samples were incubated with DAPI (1:100). Slides were mounted in VectaShield® mounting medium (Vector Laboratories) and visualized in a confocal microscope (Leica TCS SPE). Image processing was performed with LAS X software.

Statistical Analysis

Statistical analysis was performed using GraphPad Prism software (San Diego, CA, USA, v8 for Windows). A two-tailed, paired Student's *t* test was used to compare laboratory results before and after decellularization. Values are presented as the mean ± standard deviation or median and range. Differences were considered significant at $p < 0.05$.

Results

Obtaining the Liver Scaffold

The long period to decellularize a whole pig liver, which weighs approximately 1.5 kg, is a significant challenge for 3D organ engineering. In this scenario, we decellularized the porcine livers by anterograde perfusion to achieve a shorter period of decellularization. Porcine livers were perfused with the SD protocol solutions and became increasingly translucent with the dissolution of the cells. All cell remounts and nuclei were removed from the liver scaffold and we observed the remaining original liver architecture after the decellularization process (Fig. 1).

Decellularization Protocol Preserves ECM Proteins

Total cell removal with the SD protocol was further confirmed by histological evaluation with H&E (Fig. 2a, c) and Sirius red (Fig. 2b, d) staining. H&E and Sirius red staining showed no evidence of cellular remnants in the ECM (Fig. 2c, d). In addition, the overall liver tissue architecture, based on the presence of the central vein, appeared fully preserved as shown by Sirius red and immunostaining for collagens in the livers treated with the SD protocol (Fig. 2d, f, h). Immunostaining for collagens III and IV was used to evaluate the preservation of the liver structural components after decellularization (Fig. 2f, h) and showed that the collagens III and IV were indeed preserved after the process. To this end, the liver scaffold was compared with the porcine liver tissue with cells. The analysis showed that the structure of ECM was preserved, as indicated by the sinusoidal trabecular meshwork

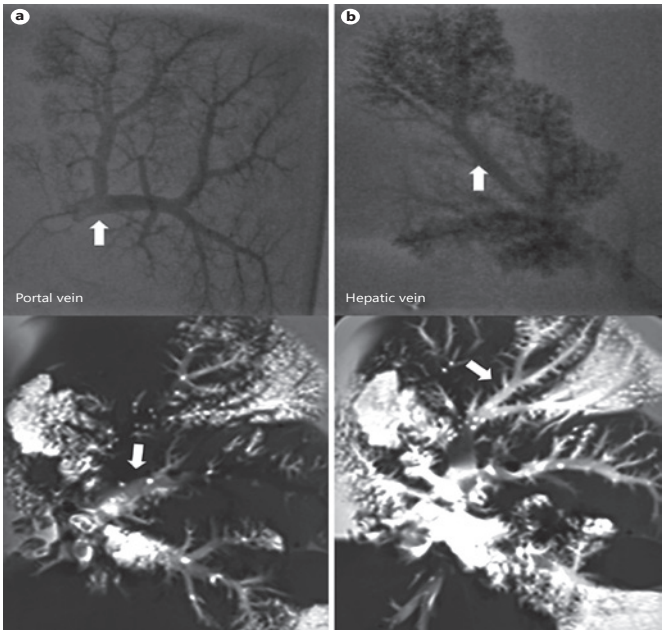

Fig. 3. Digital subtraction angiography (DSA) of decellularized liver. DSA showed an intact framework of the portal (**a**) and hepatic vein (**b**) (represented by arrows) systems with sparse emersion of contrast agent at the distal ends of the intra-hepatic capillaries despite complete removal of the vascular endothelial cells.

(Fig. 2e, g). The total GAG measured in the decellularized liver tissue was reduced (0.272 ± 0.0090 μg/mg of dry tissue) when compared to the control (0.355 ± 0.045 μg/mg of dry tissue) (Fig. 2i).

Decellularization Preserves Intact Vascular Network

To evaluate the integrity of the vascular system within the decellularized liver scaffold, DSA was performed. Iodine contrast agent (Henetix) was infused through the portal vein and via the intrahepatic vena cava. Infusion of the contrast agent showed an intact framework of the portal (Shown in Fig. 3a) and hepatic vein (Fig. 3b) systems, with a sparse emersion of the contrast agent at the distal ends of the intrahepatic capillaries despite complete removal of the vascular endothelial cells.

Decellularization Preserves 3D Ultrastructure

The preservation of the scaffold 3D ultrastructure is fundamental to allow cell adhesion and survival during recellularization. We evaluated the degree of preservation after our novel decellularization protocol using SD by performing transmission electron microscopy (TEM) of the liver scaffold in comparison to cadaveric livers with

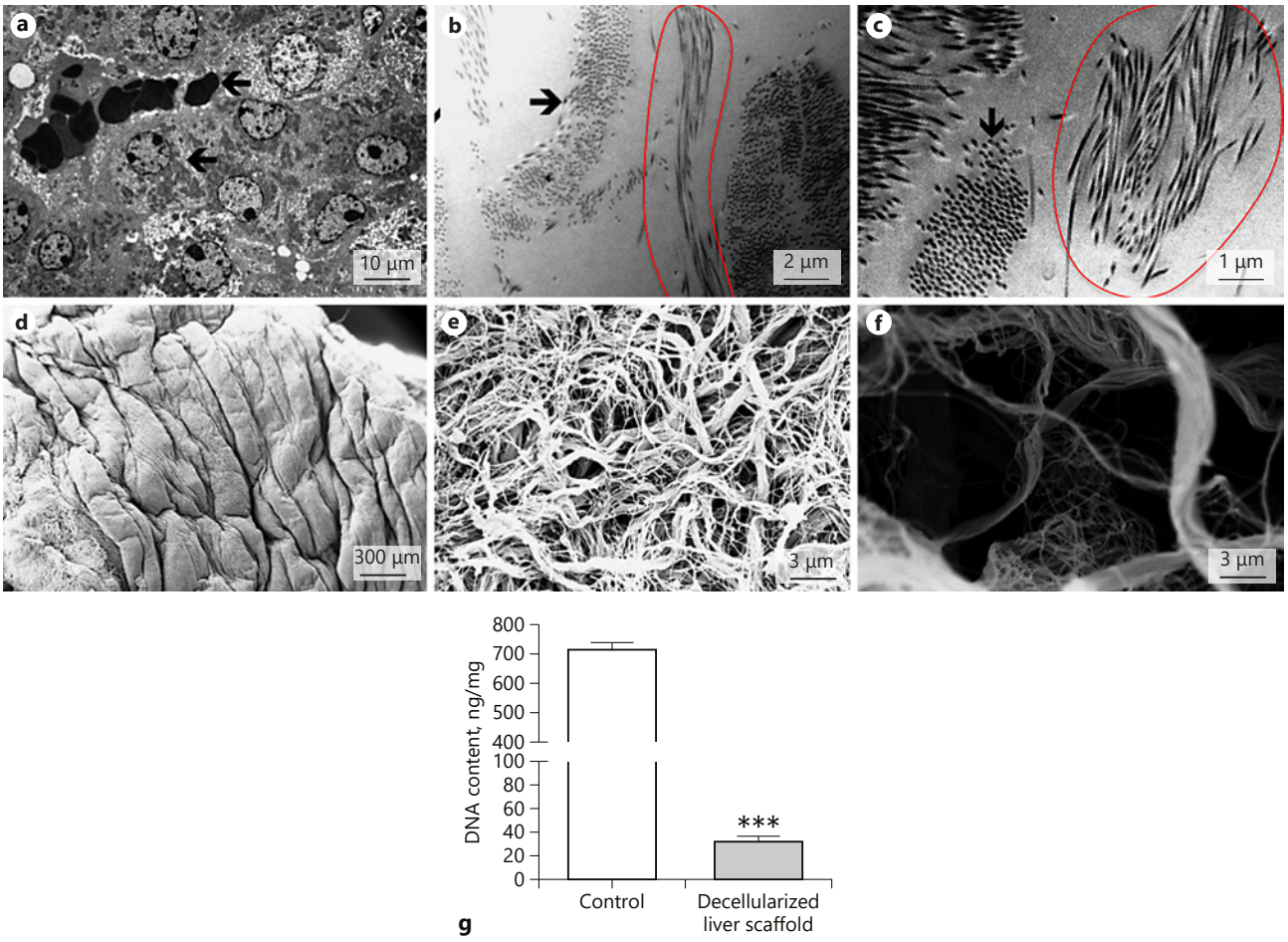

Fig. 4. Ultrastructural characterization of normal and decellularized porcine liver tissues. TEM images show the parenchyma from liver (**a**) and decellularized scaffolds by the protocol described in minor (**b**) and major (**c**) magnification. Collagen fibers are indicated with black arrows and involved by red circle. **b**, **c** The absence of cells and nuclei and the presence of collagen fibers (black arrow) were observed in scaffolds obtained after SD protocol. SEM images show the extracellular matrix within the parenchyma of normal liver (**d**) and decellularized liver in minor (**e**) and major (**f**) magnification. **g** DNA quantification shows significant reductions in DNA content using SD reagent compared to the normal liver. Each value expresses the mean of 3 samples ($n = 3$) ± SD. *** $p \leq 0.001$ vs. control.

cells. TEM images showed the absence of cells and nuclei (Fig. 4b, c) and the presence of collagen fibers in the SD-treated livers was also observed (arrow and red circle) when compared to the normal liver with cells (Fig. 4a).

Using scanning electron microscopy (SEM), we evaluated the impact of the decellularization protocol on the 3D architecture and microstructure of the decellularized porcine liver ECM when compared to the control liver with cells (Fig. 4d). The overall microstructure of the SD-treated liver tissue was intact. Open spaces in the liver previously occupied by hepatic parenchymal cells were seen in the SEM image from the SD-treated sample (Fig. 4e, f).

The absence of viable cells in the ECM scaffold in the SD-treated livers was also confirmed by the quantification of DNA, demonstrating a significant DNA reduction (27.3 ± 6.38 ng/mg) compared to the control (697 ± 32.08 ng/mg) (Fig. 4g).

Bioscaffold Cell Seeding

Cell seeding in slices of the decellularized scaffold (decellularized liver scaffold slices) (Fig. 5a) showed cells at-

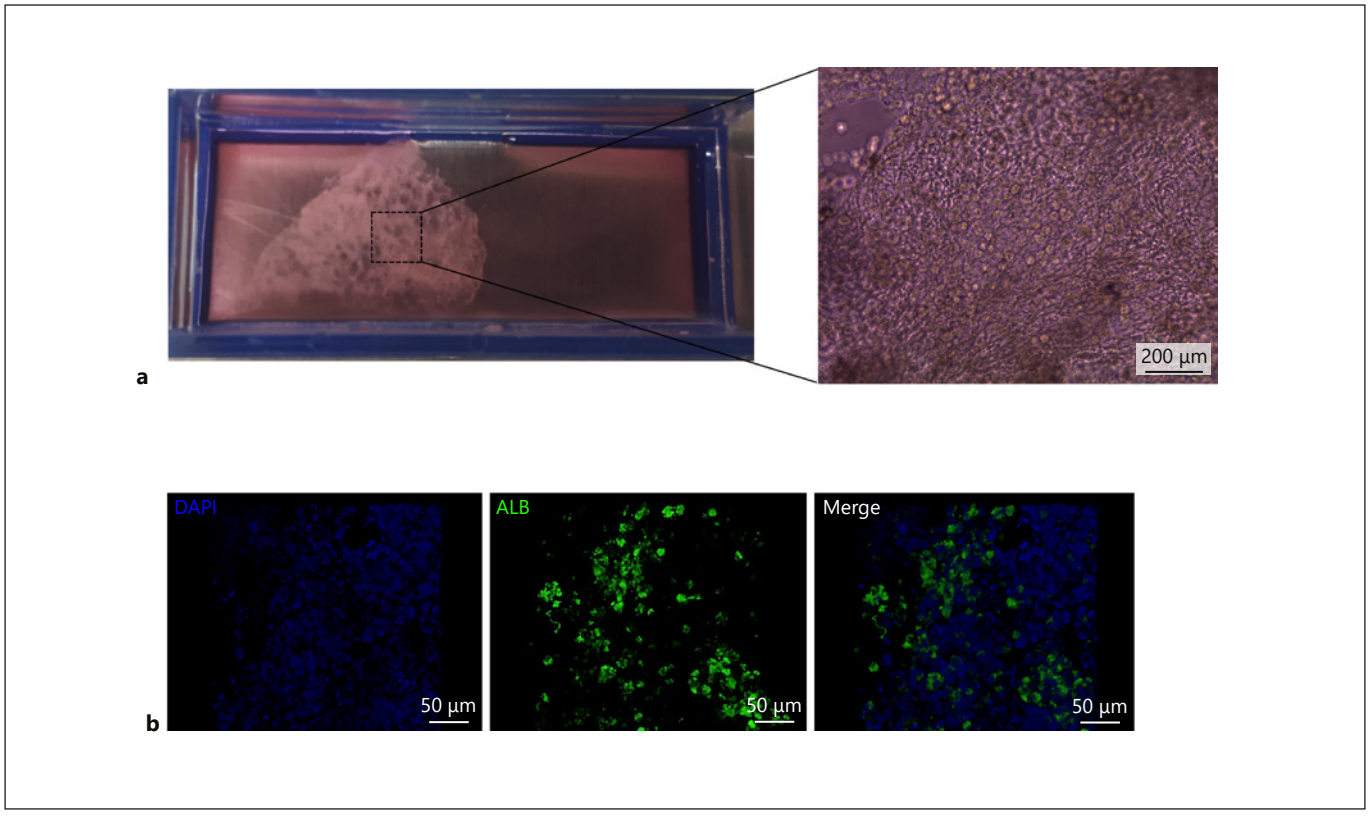

Fig. 5. Cell seeding over the slice of porcine liver matrix. **a** Light microscopy showing the slice and HepG2 cells seeded in the decellularized liver slice. **b** HepG2 nuclei staining with DAPI (blue) and albumin (green), indicating that the cells were in the ECM after 7 days' culture over the slice.

tached to the scaffold 7 days in culture when using the SD decellularization protocol. Immunofluorescence analysis showed the presence of albumin protein in the cells, indicating that HepG2 cells were producing this important liver protein (Fig. 5b) when cocultured with the SD-derived matrix. The positive control also showed the presence of this protein (online suppl. Fig. 1a–c) and the negative control showed the absence of nuclei and albumin protein (online suppl. Fig. 1b–d).

Discussion

This study describes an effective protocol that enabled complete decellularization of a whole porcine liver, resulting in a liver scaffold with preserved tissue integrity within 3 days. This is a marked improvement over existing decellularization methodologies for whole porcine liver. We also showed that the decellularized matrix enabled the attachment of cells. These cells produced albumin, an important liver protein, showing that the living cells were functional.

Pigs are currently considered to be the most feasible source of organs for human xenotransplantation because of their anatomical and physiological similarities to humans, and their relative ease of breeding in large numbers [Wang et al., 2009]. The first successful decellularization of porcine liver tissue was reported in 2004; the test was conducted with small pigs using ammonium hydroxide and Triton as detergents [Lin et al., 2004]. Since then, other protocols that enable successful decellularization have been described for other liver sources [Uygun et al., 2011; Kajbafzadeh et al., 2013; Nari et al., 2013; Agarwal et al., 2019]. However, these studies all used the livers from smaller pigs, or else goats or sheep, i.e., they could not be transplanted into humans who obviously require human-sized organs.

The livers of pigs that weigh around 72 kg are the most favorable for use for human xenotransplantation [Wang et al. 2009; Nykonenko et al., 2017]. However, most decel-

lularization protocols of whole porcine livers from larger-sized pigs require from several days to weeks for complete cell removal [Lin et al., 2004].

Distinct from other decellularization protocols using small-sized pigs [Lin et al., 2004] and therefore requiring less time for the process of decellularization, our protocol for whole porcine livers was established in larger pigs weighing 120 ± 4.2 kg which makes the transition to human livers feasible. Besides, our liver scaffold is relevant for clinical use, e.g., for split-liver transplantation which provides for ≥2 patients. Split-liver transplantation is a surgical method used to reduce waiting-list mortality. According to Valentino et al. [2019] and Lauterio et al. [2015], the graft can be separated into 2 viable sections that can be transplanted into 2 recipients. Here, our bioengineered scaffold derived from a large liver could be surgically segmented to increase the available number of grafts. Our protocol using livers weighing approximately 1.5 kg is an ideal option for increasing the number of available liver grafts to reduce the waiting list for transplantation.

Our novel SD decellularization protocol, based on anterograde perfusion for fast decellularization, resulted in the complete removal of immunogenic cellular materials while preserving the 3D architecture and essential ECM proteins of this organ. The resulting liver scaffold was robust, easily handled without disintegration or rupture, and tissue flexibility was retained. These data were further confirmed by SEM images which showed an extremely well-preserved 3D microanatomy of the portal tracts and liver lobules as well as conservation of a 3D meshwork of connective-tissue fibers around hepatocyte-free spaces.

The choice of detergent plays an important role in the decellularization process as it may impact the preservation of important organ structures and the effectiveness of the process [Faulk et al., 2015]. SDS can damage ECM components and its use in human tests is still controversial [Keane et al., 2016]. We developed a protocol using the ionic detergent SD, based on a previously published report that used porcine hearts [Remlinger et al., 2012]. Our protocol using SD achieved complete decellularization of a porcine liver without altering the 3D ECM structure of the organ. Importantly, the SD concentration used in the protocol was lower (4%) than that used in the clinical setting (5%) [Rotunda et al., 2004], making it a promising method for modification in human organ transplantations.

Maintaining ECM protein composition and concentration and an intact vasculature are necessary factors for cell attachment, growth, and differentiation. Immunostaining of the critical ECM components showed that collagen III and collagen IV were located in the basement membrane of bile ducts and in the arterial and venous vessels and were sparsely distributed in the Disse space. These findings indicate that the main structural proteins of the liver lobules and portal space were preserved. Although a few liver lobules lost their configuration, most of them maintained the hexagonal arrangement delineated by connective tissue that is characteristic of porcine livers.

Our results also demonstrated that, on average, >77% of GAG was conserved in the decellularized porcine liver. These results are comparable to those of other studies demonstrating that this loss is normal, as GAG is associated with cellular membranes and the cells are solubilized in the decellularization process [Yagi et al., 2013; Wang et al., 2015].

Cell removal was also evaluated by the amount of DNA according to the criterion established by Crapo et al. [2011], who indicated that for efficient decellularization, scaffolds should have <50 ng/mg of DNA. Our data demonstrated that SD was efficient in removing the cells, presenting an average DNA content of 27.3 ± 6.38 ng/mg [Crapo et al., 2011].

A limitation of this work is the absence of 2e critical characteristics of the matrix, namely, protein components and mechanical force [Uygun et al., 2010; Crapo et al., 2011; Wu et al., 2015; White et al., 2017]. These characteristics are relevant and further experiments are necessary to progress towards potential clinical applications. It is important to emphasize that our goal was to produce a liver scaffold which was able to be used for coculture with cells. The liver bioscaffold produced here could be used to substitute existing synthetic matrix, as already described in several studies [Godoy et al., 2013; Brown and Badylak, 2014; Wang et al., 2017].

In summary, we have described a modified protocol to decellularize a whole porcine liver within 72 h that successfully preserved the 3D architecture and kept the hepatic ECM components intact so that liver cells could be supported.

The availability of a shorter (72 h) and cost-effective protocol for whole porcine liver decellularization represents an important advance towards the translation of human-sized bioartificial liver replacements for tissue engineering and organ replacement. Donor livers not suitable for transplantation contain ECM that could be exploited for use in bioartificial liver engineering applications using the decellularization protocol described here. The next step forward will be to recellularize a liver lobe

after whole porcine liver decellularization with hepatocytes; from this, we would gain insight into using bioartificial liver scaffolds with the potential for clinical use.

Acknowledgments

The authors sincerely thank Adriana A. Piquet who collaborated for the GAG experiments.

Statement of Ethics

This study was approved by the Institutional Animal Care and Use Committee (IACUC) of the Animal Research Ethics Committee of the Albert Einstein Hospital, São Paulo, Brazil (reg. No. Einstein 2017-14). All experiments were performed in accordance with the NIH guide for the care and use of laboratory animals.

Conflict of Interest Statement

There are no conflicts of interest.

Funding Sources

This study was supported by the Brazilian Council for Scientific and Technological Development (CNPq), the Rio de Janeiro State Research Foundation (FAPERJ), the Department of Science and Technology (DECIT)/Brazilian Ministry of Health, and the Coordination for the Improvement of Higher Education Personnel (CAPES).

Author Contributions

L.A.P.F. and G.D.S. designed the research and were involved with all experiments described here. M.L.D. was responsible for writing this paper with L.A.P.F. V.H. performed all procedures with L.A.P.F. C.P. performed immunofluorescence. C.H.-M. performed immunohistochemistry. D.B.P. and E.L. performed the digital subtraction angiography experiments. P.A.S.M. performed the GAG analysis. P.R.d.O.S. and A.C.G. donated all the porcine livers used in this work. A.C.C.d.C. revised the manuscript. R.C.d.S.G. was the principal investigator and was responsible for ideas, designing the work, the objectives, manuscript revision, and coordination.

References

Agarwal T, Maiti TK, Ghosh SK. Decellularized caprine liver-derived biomimetic and pro-angiogenic scaffolds for liver tissue engineering. Mater Sci Eng C. 2019 May;98:939–48.

Ansari T, Southgate A, Obiri-Yeboa I, Jones LG, Greco K, Olayanju A, et al. Development and Characterization of a Porcine Liver Scaffold. Stem Cells Dev. 2020 Mar;29(5):314–26.

Baptista PM, Siddiqui MM, Lozier G, Rodriguez SR, Atala A, Soker S. The use of whole organ decellularization for the generation of a vascularized liver organoid. Hepatology. 2011 Feb;53(2):604–17.

Barakat O, Abbasi S, Rodriguez G, Rios J, Wood RP, Ozaki C, et al. Use of decellularized porcine liver for engineering humanized liver organ. J Surg Res. 2012 Mar;173(1):e11–25.

Bellezzia MA, Cruz FF, Martins V, de Castro LL, Lopes-Pacheco M, Vilanova EP, et al. Impact of different intratracheal flows during lung decellularization on extracellular matrix composition and mechanics. Regen Med. 2018 Jul;13(5):519–30.

Brown BN, Badylak SF. Extracellular matrix as an inductive scaffold for functional tissue reconstruction. Transl Res. 2014 Apr;163(4):268–85.

Bühler NE, Schulze-Osthoff K, Königsrainer A, Schenk M. Controlled processing of a full-sized porcine liver to a decellularized matrix in 24 h. J Biosci Bioeng. 2015 May;119(5):609–13.

Burk J, Erbe I, Berner D, Kacza J, Kasper C, Pfeiffer B, et al. Freeze-thaw cycles enhance decellularization of large tendons. Tissue Eng Part C Methods. 2014 Apr;20(4):276–84.

Cebotari S, Tudorache I, Jaekel T, Hilfiker A, Dorfman S, Ternes W, et al. Detergent decellularization of heart valves for tissue engineering: toxicological effects of residual detergents on human endothelial cells. Artif Organs. 2010 Mar;34(3):206–10.

Cooper DK, Dou KF, Tao KS, Yang ZX, Tector AJ, Ekser B. Pig Liver Xenotransplantation: A Review of Progress Toward the Clinic. Transplantation. 2016 Oct;100(10):2039–47.

Crapo PM, Gilbert TW, Badylak SF. An overview of tissue and whole organ decellularization processes. Biomaterials. 2011 Apr;32(12):3233–43.

Faulk DM, Wildemann JD, Badylak SF. Decellularization and cell seeding of whole liver biologic scaffolds composed of extracellular matrix. J Clin Exp Hepatol. 2015 Mar;5(1):69–80.

Godoy P, Hewitt NJ, Albrecht U, Andersen ME, Ansari N, Bhattacharya S, et al. Recent advances in 2D and 3D in vitro systems using primary hepatocytes, alternative hepatocyte sources and non-parenchymal liver cells and their use in investigating mechanisms of hepatotoxicity, cell signaling and ADME. Arch Toxicol. 2013 Aug;87(8):1315–530.

Jakus AE, Laronda MM, Rashedi AS, Robinson CM, Lee C, Jordan SW, et al. "Tissue Papers" from Organ-Specific Decellularized Extracellular Matrices. Adv Funct Mater. 2017 Sep;27(3):1700992.

Johnson RJ, Bradbury LL, Martin K, Neuberger J; UK Transplant Registry. Organ donation and transplantation in the UK-the last decade: a report from the UK national transplant registry. Transplantation. 2014 Jan;97(97 Suppl 1):S1–27.

Keane TJ, Saldin T, Badylak SF. Decellularization of mammalian tissue: preparing extracellular matrix bioscaffolds. In: Tomlins P, editor. Characterisation and Design of Tissue Scaffolds. Sawston: Woodhead; 2016. pp. 75–103.

Kajbafzadeh AM, Javan-Farazmand N, Monajemzadeh M, Baghayee A. Determining the optimal decellularization and sterilization protocol for preparing a tissue scaffold of a human-sized liver tissue. Tissue Eng Part C Methods. 2013 Aug;19(8):642–51.

Ko IK, Peng L, Peloso A, Smith CJ, Dhal A, Deegan DB, et al. Bioengineered transplantable porcine livers with re-endothelialized vasculature. Biomaterials. 2015 Feb;40:72–9.

Lang R, Stern MM, Smith L, Liu Y, Bharadwaj S, Liu G, et al. Three-dimensional culture of hepatocytes on porcine liver tissue-derived extracellular matrix. Biomaterials. 2011 Oct;32(29):7042–52.

Lauterio A, Di Sandro S, Concone G, De Carlis R, Giacomoni A, De Carlis L. Current status and perspectives in split liver transplantation. World J Gastroenterol. 2015;21:11003–15.

Lin P, Chan WC, Badylak SF, Bhatia SN. Assessing porcine liver-derived biomatrix for hepatic tissue engineering. Tissue Eng. 2004 Jul-Aug;10(7-8):1046–53.

Mirmalek-Sani SH, Sullivan DC, Zimmerman C, Shupe TD, Petersen BE. Immunogenicity of decellularized porcine liver for bioengineered hepatic tissue. Am J Pathol. 2013 Aug;183(2):558–65.

Mußbach F, Settmacher U, Dirsch O, Xie C, Dahmen U. Bioengineered Livers: A New Tool for Drug Testing and a Promising Solution to Meet the Growing Demand for Donor Organs. Eur Surg Res. 2016;57(3-4):224–39.
Nari GA, Cid M, Comín R, Reyna L, Juri G, Taborda R, et al. Preparation of a three-dimensional extracellular matrix by decellularization of rabbit livers. Rev Esp Enferm Dig. 2013 Mar;105(3):138–43.
Nonaka PN, Campillo N, Uriarte JJ, Garreta E, Melo E, de Oliveira LV, et al. Effects of freezing/thawing on the mechanical properties of decellularized lungs. J Biomed Mater Res A. 2014 Feb;102(2):413–9.
Nykonenko A, Vávra P, Zonča P. Anatomic Peculiarities of Pig and Human Liver. Exp Clin Transplant. 2017 Feb;15(1):21–6.
Ott HC, Matthiesen TS, Goh SK, Black LD, Kren SM, Netoff TI, et al. Perfusion-decellularized matrix: using nature's platform to engineer a bioartificial heart. Nat Med. 2008 Feb;14(2):213–21.
Pla-Palacín I, Sainz-Arnal P, Morini S, Almeida M, Baptista PM. Liver Bioengineering Using Decellularized Whole-Liver Scaffolds. In: Turksen K, editor. Decellularized Scaffolds and Organogenesis. New York: Humana Press; 2017. vol. 1. pp. 293–305.
Price AP, England KA, Matson AM, Blazar BR, Panoskaltsis-Mortari A. Development of a decellularized lung bioreactor system for bioengineering the lung: the matrix reloaded. Tissue Eng Part A. 2010 Aug;16(8):2581–91.
Remlinger NT, Wearden PD, Gilbert TW. Procedure for decellularization of porcine heart by retrograde coronary perfusion. J Vis Exp. 2012;70:e50059.
Rieder E, Kasimir MT, Silberhumer G, Seebacher G, Wolner E, Simon P, et al. Decellularization protocols of porcine heart valves differ importantly in efficiency of cell removal and susceptibility of the matrix to recellularization with human vascular cells [published correction appears in J Thorac Cardiovasc Surg. 2015 May;149(5):1469]. J Thorac Cardiovasc Surg. 2004 Feb;127(2):399–405.
Rotunda AM, Suzuki H, Moy RL, Kolodney MS. Detergent effects of sodium deoxycholate are a major feature of an injectable phosphatidylcholine formulation used for localized fat dissolution. Dermatol Surg. 2004 Jul;30(7):1001–8.
Sullivan DC, Mirmalek-Sani SH, Deegan DB, Baptista PM, Aboushwareb T, Atala A, et al. Decellularization methods of porcine kidneys for whole organ engineering using a high-throughput system. Biomaterials. 2012 Nov;33(31):7756–64.
Uygun BE, Price G, Saedi N, Izamis ML, Berendsen T, Yarmush M, et al. Decellularization and recellularization of whole livers. J Vis Exp. 2011 Feb;(48):2394.
Uygun BE, Soto-Gutierrez A, Yagi H, Izamis ML, Guzzardi MA, Shulman C, et al. Organ reengineering through development of a transplantable recellularized liver graft using decellularized liver matrix. Nat Med. 2010 Jul;16(7):814–20.
Valentino PL, Emre S, Geliang G, Li L, Deng Y, Mulligan D, Rodriguez-Davalos MI. Frequency of whole-organ in lieu of split-liver transplantation over the last decade: children experienced increased wait time and death. Am J Transplant. 2019;19:3114–23.
Wang PJ, Li WC, Xi GM, Wang HQ, Zhang ZH, Yao BC, et al. Biomechanical study of hepatic portal vein in humans and pigs and its value in liver transplantation. Transplant Proc. 2009 Jun;41(5):1906–10.
Wang Y, Bao J, Wu Q, Zhou Y, Li Y, Wu X, et al. Method for perfusion decellularization of porcine whole liver and kidney for use as a scaffold for clinical-scale bioengineering engrafts. Xenotransplantation. 2015 Jan-Feb;22(1):48–61.
Wang Y, Nicolas CT, Chen HS, Ross JJ, De Lorenzo SB, Nyberg SL. Recent Advances in Decellularization and Recellularization for Tissue-Engineered Liver Grafts. Cells Tissues Organs. 2017;204(3-4):125–36.
White LJ, Taylor AJ, Faulk DM, Keane TJ, Saldin LT, Reing JE, et al. The impact of detergents on the tissue decellularization process: A ToF-SIMS study. Acta Biomater. 2017 Mar;50:207–19.
Willemse J, Verstegen MM, Vermeulen A, Schurink IJ, Roest HP, van der Laan LJ, et al. Fast, robust and effective decellularization of whole human livers using mild detergents and pressure controlled perfusion. Mater Sci Eng C. 2020 Mar;108:110200.
Wu Q, Bao J, Zhou YJ, Wang YJ, Du ZG, Shi YJ, et al. Optimizing perfusion-decellularization methods of porcine livers for clinical-scale whole-organ bioengineering. BioMed Res Int. 2015;2015:785474.
Yagi H, Fukumitsu K, Fukuda K, Kitago M, Shinoda M, Obara H, et al. Human-scale whole-organ bioengineering for liver transplantation: a regenerative medicine approach. Cell Transplant. 2013;22(2):231–42.
Yang M, Chen CZ, Wang XN, Zhu YB, Gu YJ. Favorable effects of the detergent and enzyme extraction method for preparing decellularized bovine pericardium scaffold for tissue engineered heart valves. J Biomed Mater Res B Appl Biomater. 2009 Oct;91(1):354–61.
Zhang J, Zhao X, Liang L, Li J, Demirci U, Wang S. A decade of progress in liver regenerative medicine. Biomaterials. 2018 Mar;157:161–76.